Research Square

Preprints are preliminary reports that have not undergone peer review.
They should not be considered conclusive, used to inform clinical practice,
or referenced by the media as validated information.

The molecular and crystal structure of Shibasaki's (R)-ALB chiral catalyst

Simone Stampatori
University of Modena and Reggio Emilia
Nassima Yamini
University of Modena and Reggio Emilia
Valeria Iacomini
University of Modena and Reggio Emilia
Alessio Nicolini
University of Modena and Reggio Emilia
Francesca Parenti
University of Modena and Reggio Emilia
Andrea Cornia
acornia@unimore.it
University of Modena and Reggio Emilia

Research Article

Keywords: main group chemistry, axial chirality, lithium, aluminum

Posted Date: November 10th, 2026

DOI: https://doi.org/10.21203/rs.3.rs-11309138/v1

License: This work is licensed under a Creative Commons Attribution 4.0 International License.
Read Full License

Additional Declarations: No competing interests reported.

Abstract

Shibasaki's heterobimetallic compound [LiAl{()-BINOL}] and its enantiomer, often referred to as ()- and ()-ALB, respectively, are used as catalysts in asymmetric synthesis (BINOLH = 1,1'-bi(2-naphthol)). Crystalline ()- and ()-ALB are conveniently prepared by reacting LiAlH with 2 equiv. of ()- or ()-BINOLH, respectively, in THF and evaporating the solvent under vacuum. However, their molecular and crystal structures have never been reported in detail. We herein show that the as-crystallized ()-ALB material is a single-phase THF solvate containing [Al{()-BINOL}] anions, [Li(thf)] fragments bonded to one of the binolate O atoms, and a lattice THF molecule. This ion-paired structure was authenticated by single-crystal X-ray diffraction and then used as a starting point for the Rietveld refinement of the powder diffraction pattern. Crystallographic and NMR characterization data converge in indicating that the three THF molecules bonded to the Li ion withstand vacuum treatment. On NMR timescale, a single structure is detected in THF- solution, whereas CD solutions give more complex, multicomponent spectra that hint to aggregation effects.

Introduction

1,1'-Bi(2-naphthol) or $BINOLH_2$ is a popular molecular fragment with axial chirality and configurational stability, widely used as a ligand in asymmetric catalysis and as a stereogenic element in supramolecular and materials chemistry [1–5]. The heterobimetallic compound [LiAl{(*R*)-$BINOL\}_2$] and its enantiomer, first reported by Shibasaki *et al.* [6, 7], combine Lewis acidity and Brönsted basicity and are used as versatile catalysts for asymmetric reactions like Michael addition [6, 8–20], cyanation of imines [21] and aldehydes [22], and hydrophosphonylation [23–25] or hydrophosphinylation [26–29] of aldehydes. Often referred to as (*R*)- and (*S*)-ALB, they are usually obtained by reacting $LiAlH_4$ with 2 equiv. of (*R*)- or (*S*)-$BINOLH_2$, respectively, in THF at 0°C (Scheme 1). The catalyst is then either directly used as a THF solution or isolated as a white solid by solvent evaporation and redissolved as needed.

We prepared (*R*)-ALB in the course of our recent studies on green hydrosilylation catalysts, as we scrutinized a family of lithium salts soluble in nonpolar organic solvents. However, we noticed that a reliable X-ray structure is currently unavailable in the Cambridge Structural Database (CSD) [30]. The above authors evidently failed to obtain a publishable dataset, presumably due to the claimed tendency of X-ray quality crystals to decompose during the data collection [6]. Nevertheless, they structurally authenticated a related compound, namely [$Li(thf)_2$(cyh)Al{(*R*)-$BINOL\}_2$]·THF (**1**·THF), an adduct with 2-cyclohexen-1-one (cyh) and THF (CCDC 123644) [6]. This compound contains the expected bis-chelate Al^{3+} complex, a $[Li(thf)_2(cyh)]^+$ fragment interacting with one of the Al-coordinated O atoms, and a lattice THF molecule. In the same paper, Shibasaki *et al.* concluded that (*R*)-ALB might adopt a similar structure or be dimeric [6]. Since the structural plot reported in subsequent papers by the same group is apparently unsupported by a CSD entry [7, 13], we decided to fill this gap and make the structure finally available. We found that the white solid isolated from THF is [$Li(thf)_3$Al{(*R*)-$BINOL\}_2$]·0.67THF (**2**·0.67THF), a monomeric THF solvate containing a similar ion pair as that present in **1**·THF (Scheme 1).

Experimental

Materials and Instrumentation

Unless otherwise specified, manipulations were carried out using standard Schlenk techniques under Ar, or inside a dinitrogen-filled MBraun UNIlab glovebox (H_2O and O_2 < 1 ppm), with continuous gas circulation through activated charcoal, molecular sieves, and copper catalyst BASF R3-11(G). All glassware was dried at 100°C overnight before use. The activated 4 Å molecular sieves were stored in the glovebox before use. THF was pre-dried over KOH and subsequently distilled from Na/benzophenone under dinitrogen [31]. Hydrocarbon solvents (*n*-hexane and *n*-heptane) were not redistilled but simply deoxygenated and dried before use. All solvents, including THF-d_8 (Eurisotop, 99.5%D) and C_6D_6 (Eurisotop, 99.5%D), were deoxygenated through three freeze–pump–thaw cycles and stored at least overnight over activated 4 Å molecular sieves [32]. A solution of $LiAlH_4$ in THF (Sigma-Aldrich, 1 M) was titrated in quadruplicate via gas-volumetric titration (1.06 M). (*R*)-$BINOLH_2$ (Merck Life Science, 99%) was dried under vacuum (0.1–0.2 Torr) at 50°C for 7.5 h and stored in the glovebox before use.

NMR samples were prepared using 5 mm Norell® tubes, equipped with a Young valve and charged in the glovebox. The spectra were recorded at 298.0 K on Bruker Avance 400 and Avance III HD FT-NMR spectrometers operating at 400.13 and 600.13 MHz, respectively, for ^1H and processed using TopSpin 4.1.1 software [33]. Chemical shifts (δ) in the ^1H and $^{13}C\{^1H\}$ spectra are expressed in ppm downfield from Me_4Si as external standard, by calibrating the residual solvent signals as follows: for THF-d_8, 3.58 [C*H*D(2,5)] and 67.21 ppm [*C*D_2(2,5)]; for C_6D_6, 7.16 (C*H*) and 128.06 ppm (*C*H) [34]. ^7Li chemical shifts are referenced to 1 M LiCl in D_2O as external standard at 0.15 ppm. NMR data are reported as follows: chemical shift, multiplicity (d = doublet, m = multiplet), coupling constant (Hz), integration, assignment (see atom numbering in Scheme 1).

Synthesis

The synthesis was performed following the procedure reported by Shibasaki *et al.* [9, 18], with minor modifications. A solution of $LiAlH_4$ in THF (255 µL, 1.06 M, 0.270 mmol) was introduced in a Schlenk vessel equipped with a septum and diluted with further THF (2.5 mL). The Schlenk was cooled to 0°C in an ice bath and a solution of (*R*)-$BINOLH_2$ (150.8 mg, 0.527 mmol) in THF (2.5 mL) was added dropwise with continuous stirring. After effervescence had subsided (1–2 minutes), the colorless solution was stirred at 0°C under Ar for 30 minutes, then the ice bath was removed, the solution allowed to warm up to room temperature, and stirred for 1 hour under Ar. Finally, the solvent was removed under reduced pressure (0.2–0.3 Torr) at 0°C over 2 hours, providing a white solid in quantitative yield. This crude product is soluble in THF, insoluble in *n*-hexane and *n*-heptane, and highly moisture-sensitive. It can be optionally recrystallized with 88% recovery by slowly evaporating a THF/*n*-heptane solution (1:1.5 v/v, ca. 30 mg/mL) to 1/5 of the initial volume. ^1H NMR (400.13 MHz, 298.0 K, THF-d_8): δ = 7.82 (m, 8H, C4-H +

C5-H), 7.30 (d, $^{3}J_{HH}$ = 8.6, 4H, C3-H), 7.16 (m, 4H, C8-H), 7.04 (m, 8H, C6-H + C7-H), 3.62 (m, 4H, THF), 1.77 (m, 4H, THF). $^{13}C\{^{1}H\}$ NMR (100.61 MHz, 298.0 K, THF-d_8): δ = 157.0, 135.5, 129.9, 129.4, 128.4, 127.3, 125.5, 124.7, 122.7, 120.9, 68.0, 26.2. ^{7}Li NMR (155.51 MHz, 298.0 K, THF-d_8): δ = −0.7. Crystals suitable for X-ray diffraction were obtained from THF/*n*-hexane.

X-ray Crystallography

A Bruker-Nonius X8APEX diffractometer, equipped with a Mo-Kα generator, an area detector, and a Kryoflex cryostat, was used to collect single-crystal X-ray diffraction data at 200 K. Crystals were immersed in NVH oil (Jena Bioscience) and mounted on a MiTeGen Microloop™. Data collection and reduction with scaling and multi-scan absorption correction were carried out with APEX2 v1.0-22, SAINT v7.06A, and SADABS v2.10 programs [35]. Structure solution and refinement followed standard procedures based on SIR92 [36] and SHELXL-2018/3 [37] programs in WINGX v2020.2 [38]. All non-hydrogen atoms were treated anisotropically, while isotropic displacement parameters for H atoms were constrained to $U = 1.2U_{eq}$(C). When allowed to freely refine, the occupancy of the lattice THF molecule converged to 0.659(11) and was subsequently fixed to 2/3. An ellipsoid plot of the structure is presented in **Figure S1**, while crystal data and refinement parameters are gathered in Table 1. Selected bond distances and angles, and non-classical H-bond interactions are listed in Table 2 and S1, respectively.

Deposition Number 2591352 contains the supplementary crystallographic data for this paper. These data are provided free of charge by the joint Cambridge Crystallographic Data Centre and Fachinformationszentrum Karlsruhe Access Structures service.

Powder X-ray diffraction (PXRD) was carried out at room temperature (298 K) with a Malvern-Panalytical Empirean MultiCore X-ray powder diffractometer, equipped with an Empirean tube Cu LFF High Resolution (wavelength, λ = 1.54056 Å) at 40 kV and 40 mA, and with a capillary spinner sample stage rotating during the measurement (to reduce the impact of preferred orientation of the crystallites). Inside the glovebox, crystals of the compound were ground and filled into a glass capillary, which was then sealed with epoxy glue. Data collection was performed in the range 2θ = 5–50° in steps of 0.013° and with a counting time of 2000 s per step. The refinement of the model from single-crystal X-ray diffraction (CCDC 2591352) was performed by Rietveld method (2θ = 6–40°), implemented in GSAS-II [39]. Peak profiles were described by a pseudo-Voigt function fixing the instrumental parameters (U, V, W, X, and Y) to the best-fit values obtained in the same conditions for the NIST standard LaB_6 660a. The background was modeled using a Chebyschev-1 polynomial (with 12 coefficients). The refinement followed a sequential process starting from scale factor, zero, and unit cell parameters (due to the low signal/noise ratio, the background was initially fixed and then refined afterwards). Subsequently, crystallite size and microstrain were refined to account for sample-dependent peak broadening. Finally, the position and orientation of **2** and of crystallization THF (occupancy fixed to 0.67) were refined, treating both moieties as rigid bodies (R_{wp} = 2.90%, R_p = 2.21%, R_{Bragg} = 13.99%, GOF = 2.58, χ^2 = 6.63).

Table 1
Crystal data and refinement parameters for **2**·0.67THF

Radiation	**Mo-Kα (λ = 0.71073 Å)**
Chemical formula	$C_{54.67}H_{53.33}AlLiO_{7.67}$
Formula weight	866.89
T (K)	200(2)
Crystal size (mm^3)	0.04 × 0.08 × 0.23
Crystal system	triclinic
Space group	*P*1
a (Å)	9.4993(8)
b (Å)	10.8584(10)
c (Å)	12.6391(10)
α (deg)	82.984(3)
β (deg)	84.998(3)
γ (deg)	69.279(3)
V ($Å^3$)	1208.87(18)
Z	1
ρ_{calcd} ($g\ cm^{-3}$)	1.191
$2\theta_{min}/2\theta_{max}$ (deg)	5.420 / 50.862
Reflections collected/independent	11666 / 7721
№ of parameters/ restraints	595 / 3
*R*1/*wR*2 (all data)	0.0766 / 0.1521
*R*1/*wR*2 ($I > 2\sigma(I)$)	0.0534 / 0.1348
GOF	1.042
Largest diff. peak/hole ($eÅ^{-3}$)	0.369 /−0.209

Results and Discussion

Single-crystal X-ray diffraction

The product was isolated in quantitative yield by reacting stoichiometric amounts of $LiAlH_4$ and (*R*)-$BINOLH_2$ in THF at 0°C and subsequently evaporating the solvent (Scheme 1). Recrystallization of the crude product from THF/*n*-hexane afforded plate-like crystals exceedingly sensitive to solvent loss but suitable for single-crystal work at 200 K (Table 1). The resulting molecular structure is displayed in Fig. 1 and S1. The compound crystallizes in space group *P*1, with one formula unit per unit cell. The Al^{3+} ion is tetrahedrally coordinated by two chelating (*R*)-$BINOL^{2-}$ ligands with Al-O distances of 1.73–1.77 Å and O-Al-O bite angles between 104.8 and 107.4° (Table 2). The dihedral angle between the two naphthyl groups is quite similar in the two ligands, with values of 64.9 and 67.2° (evaluated from the mean planes through the C atoms only). The longest Al-O separation of 1.766(3) Å is with the O atom (O3) engaged in a coordination bond with the Li^+ ion at 1.963(9) Å. The alkali metal ion is further coordinated by three THF molecules (1.93–1.99 Å). An additional uncoordinated THF molecule was located in the lattice and refined with 2/3 occupancy. The absolute structure [Flack parameter = 0.01(11)] [40] is consistent with the occurrence of (*R*)-$BINOL^{2-}$ in the structure.

Table 2
Selected bond distances (Å) and angles (°) in **2**·0.67THF

Al1–O1	**1.734(4)**	**Li1–O3**	**1.963(9)**
Al1–O2	1.747(3)	Li1–O5	1.926(11)
Al1–O3	1.766(3)	Li1–O6	1.930(10)
Al1–O4	1.745(4)	Li1–O7	1.989(10)
O1–Al1–O2	107.35(17)	O3–Li1–O5	107.6(4)
O1–Al1–O3	118.04(18)	O3–Li1–O6	113.6(5)
O1–Al1–O4	106.18(18)	O3–Li1–O7	114.6(5)
O2–Al1–O3	104.29(16)	O5–Li1–O6	111.2(5)
O2–Al1–O4	116.70(19)	O5–Li1–O7	105.6(5)
O3–Al1–O4	104.82(16)	O6–Li1–O7	103.9(4)

Intermolecular interactions entail no classical H bonds. Crystal cohesion relies on van der Waals forces and a few C-H···O contacts (**Table S1**). These involve the aromatic CH groups of the (*R*)-$BINOL^{2-}$ ligands and the O atom of lattice THF molecules (H···*A* = 2.57–2.77 Å), as well as three CH groups of coordinated THF molecules and O1 of a neighboring complex translated along the *a* axis (H···*A* = 2.68-3.00 Å).

Powder X-ray diffraction

After recrystallization from THF/*n*-heptane, the solid gave the room-temperature PXRD pattern shown in Fig. 2 and S2 (the crude material yields an identical pattern). The successful Rietveld refinement starting

from single-crystal data at 200 K shows that both the crude and the recrystallized compound are a single phase.

NMR characterization

According to NMR characterization in THF-d_8, the vacuum dried crude product isolated from THF contains from 2.9 to 3.6 THF molecules per formula unit (**Figure S3**). This agrees with single-crystal diffraction data and suggests that only the lattice THF molecules are lost upon vacuum treatment. The simple pattern of ^{1}H NMR resonances (**Figure S3**) and the set of ten aromatic ^{13}C NMR signals (**Figure S4**) match the expectation for the C_2 symmetric (*R*)-BINOL^{2-} anion, indicating that a single structure is present on NMR timescale [11, 41]. The ^{7}Li NMR spectrum (**Figure S5**) is dominated by a singlet at −0.7 ppm. When lithium bis(trifluoromethanesulfonyl)imide (LiTFSI) is added to the solution, this Li^+ peak increases its intensity while maintaining the same position within 0.1 ppm. This suggests that ion pairing is not preserved in THF and that Li^+ is mainly present as $[Li(THF)_n]^+$ complexes. The ^{1}H, ^{13}C NMR, and ^{7}Li spectra in C_6D_6 are considerably more complex, but perfectly reproducible among different preparations. In the aromatic region, the proton spectrum shows a dominant set of very broad resonances, overlapping with a second set of six much narrower signals accounting for ca. 10% of the aromatic protons and exhibiting well resolved scalar coupling (**Figure S6**). The latter set of six signals is identical to that observed in the spectrum of crystalline $[Li_3Al\{(R)\text{-BINOL}\}_3(thf)_6]$ (**3**) dissolved in C_6D_6 [42]. The ^{13}C NMR spectrum also displays two sets of broad and narrow signals (**Figure S7**), with the latter again matching those reported for **3** in C_6D_6 [42]. The ^{7}Li NMR spectrum shows a dominant peak at −0.7 ppm accompanied by a less intense signal at 0.1 ppm (**Figure S8**). Multinuclear NMR characterization then clearly indicates that multiple species are present on NMR timescale in C_6D_6 and supports the original suggestion by Shibasaki and co-workers that the compound may oligomerize in nonpolar solvents like benzene and toluene [11].

Conclusions

Although widely used in asymmetric catalysis, the heterobimetallic compounds (*R*)- and (*S*)-ALB have been poorly characterized in the literature. In particular, only the solid-state structure of an (*R*)-ALB adduct with 2-cyclohexen-1-one is publicly available in the CSD [6]. In our work, we have used single-crystal and powder X-ray diffraction to show that the usual procedure for the synthesis of (*R*)-ALB yields a single crystalline phase, namely **2**·0.67THF. The $[Al\{(R)\text{-BINOL}\}_2]^-$ anion in the structure contains a tetrahedrally coordinated Al^{3+} ion and interacts with a $[Li(thf)_3]^+$ cation through a Li-O bond. Multinuclear NMR spectroscopy showed that **2** adopts different structures in THF-d_8 and C_6D_6 solutions, with the latter affording much more complex spectra that hint to aggregation effects. Note that tetrametallic **3**, which also contains Li^+, Al^{3+}, enantiopure (*R*)-BINOL^{2-}, and THF ligands, is not formed in the synthetic conditions used. Another compound previously authenticated in the solid state, $[Li_2Al_2\{(R)\text{-BINOL}\}_2\{(S)$-

BINOL}$_2$(thf)$_4$]·4THF [42], contains both enantiomers and is clearly not accessible starting from the enantiopure ligand.

Declarations

Supplementary Information

The online version contains supplementary material available at https://doi.org/10.1007/

Competing interests

The authors have no competing interests to declare that are relevant to the content of this article.

Funding

The PhD position of S.S was supported by the Italian Ministry of University and Research (MUR) within the PNRR (Mission 4, Component 2, Investment 3.3), through the Ministerial Decree No. 117 of March 2, 2023, and by Versalis S.p.A..

Author Contribution

All authors contributed to the study conception and design. Material preparation, data collection and analysis were performed by S.S, N.Y, and A.N. The first draft of the manuscript was written by A.C and all authors commented on previous versions of the manuscript. All authors read and approved the final version of the manuscript.

Acknowledgement

The authors acknowledge the Centro Interdipartimentale Grandi Strumenti (CIGS) of the University of Modena and Reggio Emilia for providing the X-ray diffraction and NMR facilities used in this work.

Data Availability

All data supporting the findings of this study are available within the paper and its Supplementary Information

References

1. Krajnc M, Niemeyer J (2022) BINOL as a chiral element in mechanically interlocked molecules. Beilstein J Org Chem 18:508–523. https://doi.org/10.3762/bjoc.18.53
2. Yu S, Pu L (2015) Recent progress on using BINOLs in enantioselective molecular recognition. Tetrahedron 71:745–772. https://doi.org/10.1016/j.tet.2014.11.007
3. Yu Y, Hu Y, Ning C et al (2024) BINOL-Based Chiral Macrocycles and Cages. Angew Chem Int Ed 63:e202407034. https://doi.org/10.1002/anie.202407034
4. Brunel JM (2005) BINOL: A Versatile Chiral Reagent. Chem Rev 105:857–898. https://doi.org/10.1021/cr040079g
5. Sardar B, Kumar A, Manna K (2026) Metal–organic frameworks for sustainable asymmetric catalysis. Chem Commun 62:19107–19127. https://doi.org/10.1039/D6CC03183H
6. Arai T, Sasai H, Aoe K et al (1996) A New Multifunctional Heterobimetallic Asymmetric Catalyst for Michael Additions and Tandem Michael–Aldol Reactions. Angew Chem Int Ed 35:104–106. https://doi.org/10.1002/anie.199601041
7. Shibasaki M, Sasai H, Arai T (1997) Asymmetric Catalysis with Heterobimetallic Compounds. Angew Chem Int Ed 36:1236–1256. https://doi.org/10.1002/anie.199712361
8. Charpentier M, Jauch J (2017) Metal catalysed versus organocatalysed stereoselective synthesis: The concrete case of myrtucommulones. Tetrahedron 73:6614–6623. https://doi.org/10.1016/j.tet.2017.10.011
9. Xu Y, Ohori K, Ohshima T, Shibasaki M (2002) A practical large-scale synthesis of enantiomerically pure 3-[bis(methoxycarbonyl)methyl]cyclohexanone via catalytic asymmetric Michael reaction. Tetrahedron 58:2585–2588. https://doi.org/10.1016/S0040-4020(02)00141-2
10. Rai V, Namboothiri INN (2008) Enantioselective conjugate addition of dialkyl phosphites to nitroalkenes. Tetrahedron: Asymmetry 19:2335–2338. https://doi.org/10.1016/j.tetasy.2008.10.010
11. Emori E, Iida T, Shibasaki M (1999) Catalytic Kinetic Resolution Reaction of (±)-5-Methylbicyclo[3.3.0]oct-1-ene-3,6-dione. J Org Chem 64:5318–5320. https://doi.org/10.1021/jo9904922
12. Keller E, Veldman N, Spek AL, Feringa BL (1997) Catalytic enantioselective Michael addition reactions of α-nitroesters to α,β-unsaturated ketones. Tetrahedron: Asymmetry 8:3403–3413. https://doi.org/10.1016/S0957-4166(97)00432-1
13. Arai T, Yamada YMA, Yamamoto N et al (1996) Self-Assembly of Heterobimetallic Complexes and Reactive Nucleophiles: A General Strategy for the Activation of Asymmetric Reactions Promoted by Heterobimetallic Catalysts. Chem – Eur J 2:1368–1372. https://doi.org/10.1002/chem.19960021107
14. Charpentier M, Hans M, Jauch J (2013) Enantioselective Synthesis of Myrtucommulone A. Eur J Org Chem 2013:4078–4084. https://doi.org/10.1002/ejoc.201300179
15. Ohori K, Shimizu S, Ohshima T, Shibasaki M (2000) Catalytic asymmetric synthesis of 19,20-dihydroakuammicine. Chirality 12:400–403.

https://doi.org/10.1002
/(SICI)1520-636X(2000)12:5/6<400::AID-CHIR18>3.0.CO;2-H

16. Ohshima T (2004) Enantioselective Total Syntheses of Several Bioactive Natural Products Based on the Development of Practical Asymmetric Catalysis. Chem Pharm Bull 52:1031–1052. https://doi.org/10.1248/cpb.52.1031
17. Ohshima T, Xu Y, Takita R, Shibasaki M (2004) Enantioselective total synthesis of (–)-strychnine: development of a highly practical catalytic asymmetric carbon–carbon bond formation and domino cyclization. Tetrahedron 60:9569–9588. https://doi.org/10.1016/j.tet.2004.06.141
18. Shimizu S, Ohori K, Arai T et al (1998) A Catalytic Asymmetric Synthesis of Tubifolidine. J Org Chem 63:7547–7551. https://doi.org/10.1021/jo981069g
19. Tabatabaeian K, Mamaghani M, Pourahamad A (2001) Asymmetric Michael Addition Catalyzed by Aluminum Lithium Bis-(R)-binaphthoxide. Russ J Org Chem 37:1287–1288. https://doi.org/10.1023/A:1013131621384
20. Tiano M (2020) Enantioselective Michael Addition: An Experimental Introduction to Asymmetric Synthesis. J Chem Educ 97:2291–2295. https://doi.org/10.1021/acs.jchemed.0c00164
21. Chavarot M, Byrne JJ, Chavant PY, Vallée Y (2001) Sc(BINOL)2Li: a new heterobimetallic catalyst for the asymmetric Strecker reaction. Tetrahedron: Asymmetry 12:1147–1150. https://doi.org/10.1016/S0957-4166(01)00144-6
22. Gou S, Wang J, Liu X et al (2007) Asymmetric Cyanoethoxycarbonylation of Aldehydes Catalyzed by Heterobimetallic Aluminum Lithium Bis(binaphthoxide) and Cinchonine. Adv Synth Catal 349:343–349. https://doi.org/10.1002/adsc.200600336
23. Arai T, Bougauchi M, Sasai H, Shibasaki M (1996) Catalytic Asymmetric Synthesis of α-Hydroxy Phosphonates Using the Al – Li–BINOL Complex. J Org Chem 61:2926–2927. https://doi.org/10.1021/jo960180o
24. Kolodiazhna AO, Kukhar VP, Chernega AN, Kolodiazhnyi OI (2004) Double and triple asymmetric induction in phosphaaldol reactions. Tetrahedron: Asymmetry 15:1961–1963. https://doi.org/10.1016/j.tetasy.2004.05.022
25. Yokomatsu T, Yamagishi T, Matsumoto K, Shibuya S (1996) Stereocontrolled synthesis of hydroxymethylene phosphonate analogues of phosphorylated tyrosine and their conversion to monofluoromethylene phosphonate analogues. Tetrahedron 52:11725–11738. https://doi.org/10.1016/0040-4020(96)00671-0
26. Yamagishi T, Kusano T, Yokomatsu T, Shibuya S (2002) Stereoselective Synthesis of β-Amino-α-hydroxy(allyl)phosphinates and an Application to the Synthesis of a Building Block for Phosphinyl Peptides. Synlett 2002:1471–1474. https://doi.org/10.1055/s-2002-33529
27. Yamagishi T, Yokomatsu T, Suemune K, Shibuya S (1999) Enantioselective synthesis of α-hydroxyphosphinic acid derivatives through hydrophosphinylation of aldehydes catalyzed by Al-Li-BINOL complex. Tetrahedron 55:12125–12136. https://doi.org/10.1016/S0040-4020(99)00709-7

28. Yamagishi T, Suemune K, Yokomatsu T, Shibuya S (2001) Diastereoselective synthesis of chiral β-amino-α-hydroxy- H -phosphinates through hydrophosphinylation of α-amino aldehydes. Tetrahedron Lett 42:5033–5036. https://doi.org/10.1016/S0040-4039(01)00911-X
29. Yamagishi T, Suemune K, Yokomatsu T, Shibuya S (2002) Asymmetric synthesis of β-amino-α-hydroxyphosphinic acid derivatives through hydrophosphinylation of α-amino aldehydes. Tetrahedron 58:2577–2583. https://doi.org/10.1016/S0040-4020(02)00136-9
30. Groom CR, Bruno IJ, Lightfoot MP, Ward SC (2016) The Cambridge Structural Database. Acta Crystallogr Sect B Struct Sci Cryst Eng Mater 72:171–179. https://doi.org/10.1107/S2052520616003954
31. Simas ABC, Pereira VLP, Barreto CB Jr et al (2009) An expeditious and consistent procedure for tetrahydrofuran (THF) drying and deoxygenation by the still apparatus. Quim Nova 32:2473–2475. https://doi.org/10.1590/S0100-40422009000900042
32. Armarego WLF (2017) Purification of laboratory chemicals, 8th edn. Butterworth-Heinemann, Oxford, UK
33. Bruker (2020) TopSpin 4.1.1. Bruker AXS Inc., Madison, Wisconsin, USA
34. Fulmer GR, Miller AJM, Sherden NH et al (2010) NMR Chemical Shifts of Trace Impurities: Common Laboratory Solvents, Organics, and Gases in Deuterated Solvents Relevant to the Organometallic Chemist. Organometallics 29:2176–2179. https://doi.org/10.1021/om100106e
35. Bruker (2012) APEX2, SADABS, SAINT. Bruker-AXS Inc., Madison, Wisconsin, USA
36. Altomare A, Cascarano G, Giacovazzo C et al (1994) SIR 92 – a program for automatic solution of crystal structures by direct methods. J Appl Crystallogr 27:435–435. https://doi.org/10.1107/S002188989400021X
37. Sheldrick GM (2015) Crystal structure refinement with SHELXL. Acta Crystallogr Sect C Struct Chem 71:3–8. https://doi.org/10.1107/S2053229614024218
38. Farrugia LJ (2012) WinGX and ORTEP for Windows: an update. J Appl Crystallogr 45:849–854. https://doi.org/10.1107/S0021889812029111
39. Toby BH, Von Dreele RB (2013) GSAS-II: the genesis of a modern open-source all purpose crystallography software package. J Appl Crystallogr 46:544–549. https://doi.org/10.1107/S0021889813003531
40. Parsons S, Flack HD, Wagner T (2013) Use of intensity quotients and differences in absolute structure refinement. Acta Crystallogr Sect B Struct Sci Cryst Eng Mater 69:249–259. https://doi.org/10.1107/S2052519213010014
41. Arai T, Sasai H, Yamaguchi K, Shibasaki M (1998) Regioselective Catalytic Asymmetric Reaction of Horner–Wadsworth–Emmons Reagents with Enones: The Odyssey of Chiral Aluminum Catalysts. J Am Chem Soc 120:441–442. https://doi.org/10.1021/ja973064r
42. Nöth H, Schlegel A, Suter M (2001) A study of Noyori's reagent. J Organomet Chem 621:231–241. https://doi.org/10.1016/S0022-328X(00)00843-3

Figures

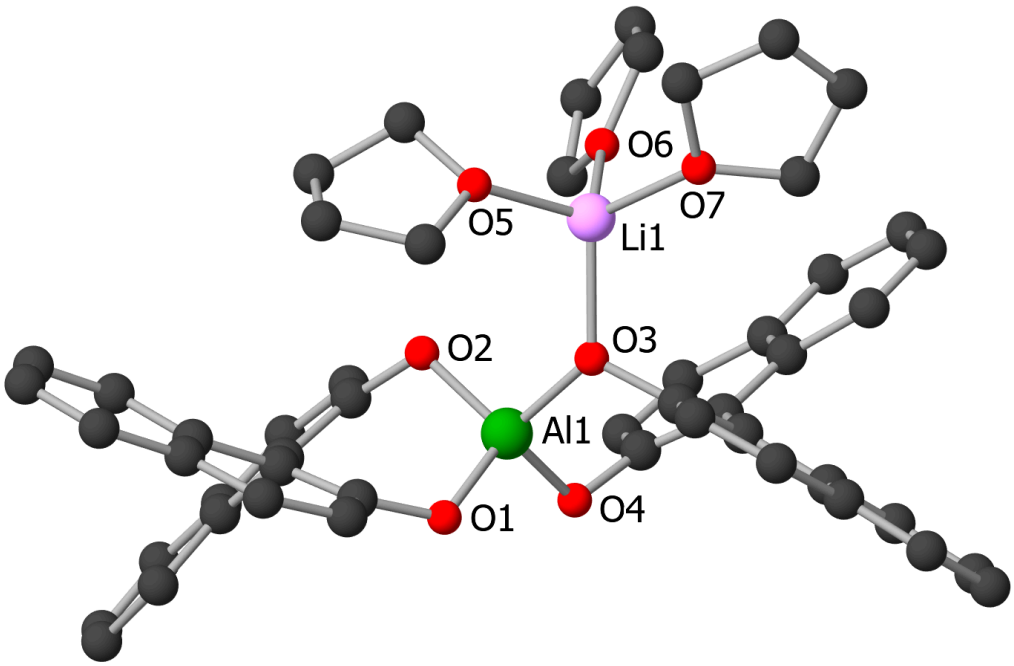


Figure 1

Ball-and-stick view of the structure of **2**, omitting H atoms. Color code: Al = green, Li = light purple, O = red, C = gray. The planarity of some THF molecules is a consequence of unresolved disorder effects

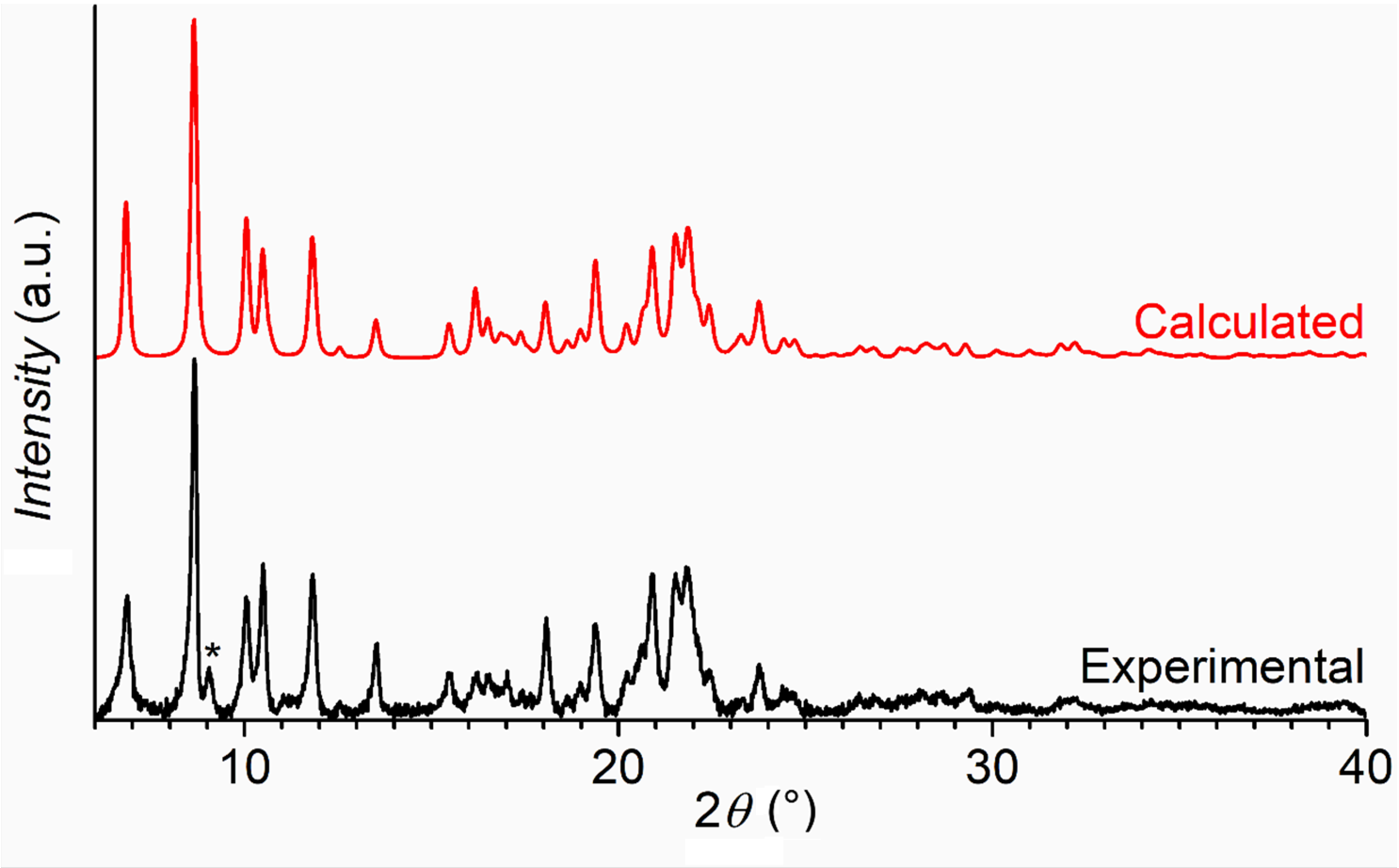


Figure 2

Experimental (black) and calculated (red) PXRD patterns for **2**·0.67THF (after background subtraction). The peak marked with an asterisk arises from an unidentified impurity

Supplementary Files

This is a list of supplementary files associated with this preprint. Click to download.

- ALB061026SI.pdf
- Scheme1.tif